

Inspired GWO-based Multilevel Thresholding for Color Images Segmentation via M. Masi Entropy

I Made Satria Bimantara^{*1}, I Wayan Supriana², I Komang Arya Ganda Wiguna³, Ida Bagus Gede Sarasvananda⁴

Informatics Department, Faculty of Mathematics and Natural Sciences, Universitas Udayana
Jl. Raya Kampus Unud Bukit Jimbara, Badung 80361, Bali, Indonesia
Email: ¹satriabimantara@unud.ac.id, ²wayan.supriana@unud.ac.id, ³arya.ganda@unud.ac.id,
⁴sarasvananda@unud.ac.id

Abstrak. *Multilevel Thresholding untuk Segmentasi Citra Berwarna berbasis Inspired GWO dengan M. Masi Entropy.* Segmentasi citra sangat penting dalam pemrosesan citra dan visi komputer, dengan Multilevel Thresholding Image Segmentation Problem (ML-ISP) yang menawarkan solusi tangguh untuk citra kompleks. Namun, penerapan ML-ISP secara efektif pada citra berwarna RGB masih menjadi tantangan karena kompleksitas komputasi dan keterbatasan algoritma optimasi tradisional seperti Grey Wolf Optimizer (GWO). Studi ini mengusulkan Inspired Grey Wolf Optimizer (IGWO) untuk mengatasi masalah ini dan meningkatkan ML-ISP untuk citra berwarna RGB. Stabilitas kinerja IGWO dievaluasi secara komprehensif menggunakan tiga fungsi objektif yang berbeda: metode Otsu, Kapur Entropy, dan M. Masi Entropy. Analisis kualitatif dan kuantitatif, menggunakan PSNR, SSIM, dan UQI, dilakukan pada citra acuan. Hasil secara konsisten menunjukkan bahwa IGWO, khususnya dengan M. Masi Entropy, mencapai kualitas segmentasi yang unggul. Penelitian ini menggabungkan penyetulan hiperparameter berbasis GridSearch. Temuan ini menyoroti efektivitas dan ketahanan pendekatan IGWO yang diusulkan untuk tugas ML-ISP kompleks pada citra berwarna.

Keywords: *Inspired Grey Wolf Optimizer, Multilevel Thresholding Segmentasi Citra Berwarna, Metode Otsu, Kapur Entropy, M. Masi Entropy*

Abstract. *Image segmentation is crucial in image processing and computer vision, with multilevel thresholding (ML-ISP) offering robust solutions for complex images. However, effectively applying ML-ISP to RGB color images remains a challenge due to computational complexity and the limitations of traditional optimization algorithms, such as the Grey Wolf Optimizer (GWO). This study proposes an Inspired Grey Wolf Optimizer (IGWO) to address these issues and enhance ML-ISP for RGB color images. The performance stability of IGWO is comprehensively evaluated using three distinct objective functions: the Otsu method, the Kapur Entropy, and the M. Masi Entropy. Qualitative and quantitative analyses using PSNR, SSIM, and UQI were conducted on benchmark images. Results consistently demonstrate that IGWO, particularly with M. Masi Entropy, achieves superior segmentation quality. This research incorporates GridSearch-based hyperparameter tuning. The findings highlight the effectiveness and robustness of the proposed IGWO approach for complex ML-ISP tasks on color images.*

Kata Kunci: *Inspired Grey Wolf Optimizer, Multilevel Color Image Thresholding, Otsu Method, Kapur Entropy, M. Masi Entropy*

1. Introduction

Image analysis is an essential process in computer vision, involving image segmentation. Thresholding is a simple and efficient segmentation technique that determines optimal threshold values based on pixel intensities [1], [2]. However, multilevel thresholding (ML-ISP) is more challenging. Non-parametric approaches such as Otsu's method, Kapur entropy, and minimal cross entropy are effective for bi-level thresholding of grayscale images. These methods often become ineffective and computationally complex [1], [2], [3] when extended to ML-ISP, particularly as the number of thresholds increases.

Entropy plays a crucial role in optimizing ML-ISP, a complex problem that requires metaheuristic optimization algorithms based on swarm intelligence (SI) [3], [4]. Otsu, Kapur, and M. Masi entropy techniques have been used in various optimization methods, demonstrating superior efficiency and accuracy compared to exhaustive search and traditional evolutionary algorithms. For instance, the Otsu method has been used with MFO [5], KHO [4], WOA [5], GWO [6], and improved WOA [4]. Kapur Entropy has been explored with WOA-SMA [7], a multistage hybrid SI method [3], DA [8], GWO [6], and KHO [4], while M. Masi Entropy has been tested with GWO [1] and PSO [8].

Existing SI-based ML-ISP research often focuses on grayscale images [1], overlooking color information. The No Free Lunch (NFL) theorem suggests that no single optimization algorithm is universally optimal. Existing SI approaches often suffer from slow convergence, premature convergence, and susceptibility to local optima, leading to suboptimal segmentation quality [2], [3]. Evaluating performance across multiple objective functions is crucial for consistency and robustness.

To address these limitations, this study proposes an Inspired Grey Wolf Optimizer (IGWO) for solving ML-ISP on RGB color images, enhancing performance over traditional population-based algorithms. IGWO's non-linear adjustment strategy and modified wolf position update mechanism balance exploration and exploitation. IGWO was chosen for its superior performance compared to conventional population-based algorithms. Benchmark images from BSD300 Berkeley and USC-SIPI demonstrate its efficacy, assessing PSNR, SSIM, and UQI.

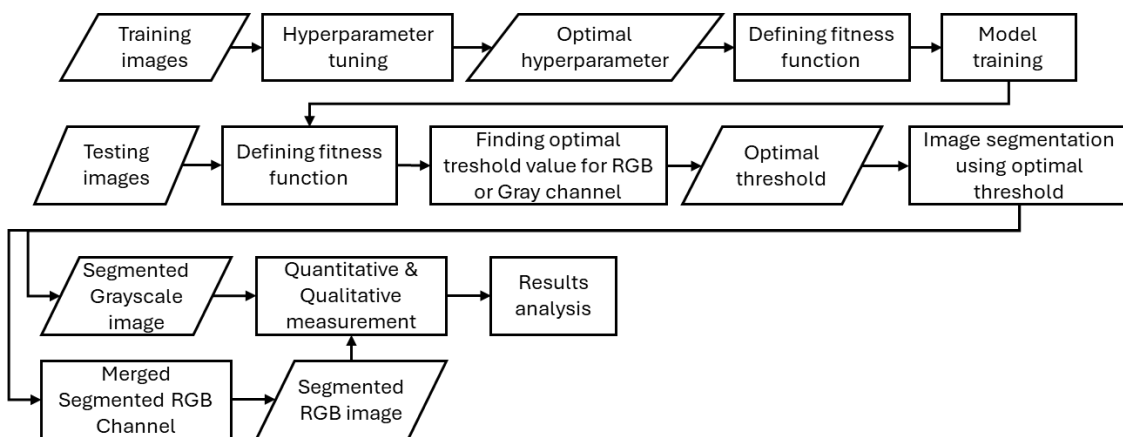


Figure 1. Research flowchart of experiment

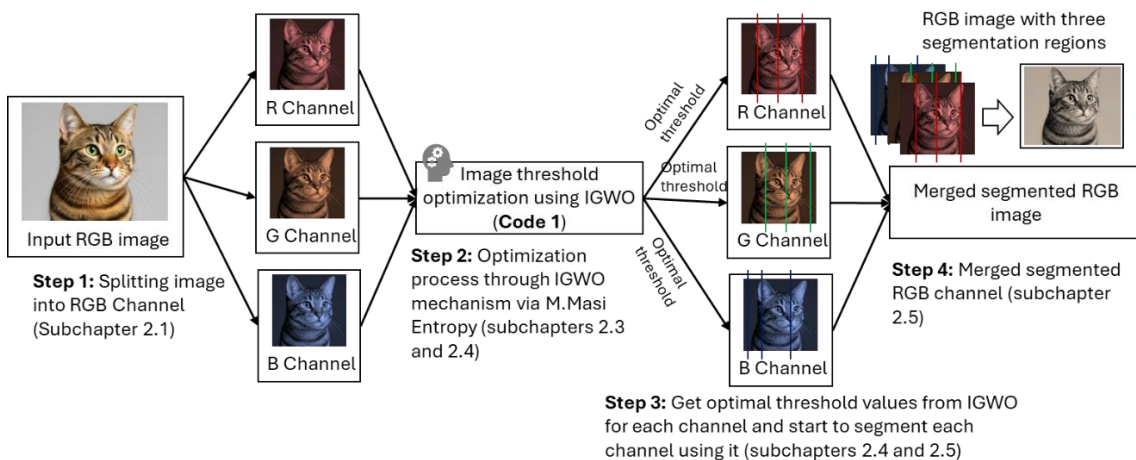


Figure 2. An intuitive visual representation of multilevel thresholding applied to color image segmentation using IGWO

2. Research Methodology

As shown in Figure 1, this section outlines the procedures used to address the research objectives and the dataset used in the study. A clear visual overview of the entire process for resolving ML-ISP using the proposed IGWO method is provided in Figure 2. We make reference to the objective functions of the Otsu, Kapur, and M. Masi entropy approaches, as well as the ML-ISP problem, to the findings of earlier studies [9].

2.1 Dataset

This study used a common benchmark dataset, the Berkeley Segmentation Dataset¹ (BSDS300), and the USC-SIPI image database². Six images serve as test data (retrieved from USC-SIPI), while ten images serve as training data (retrieved from BSDS300), as shown in Table 1. These files were selected for their multimodal histogram features, which enable the objective selection of each model's optimal hyperparameters. The training data is used for the ML-ISP IGWO model construction, including hyperparameter tuning for each model. The performance of the proposed method is evaluated using the test data. The histogram of the test data's pixel intensities is shown in Figure 3.

Table 1. Benchmark images used in this experiment

Type	Filename	Dimension (pixels)	Colorspace
Testing	House – 4.1.05	512x512	Color (24 bits/pixel)
Testing	Splash – 4.2.01	512x512	Color (24 bits/pixel)
Testing	Mandrill (a.k.a. Baboon) – 4.2.03	512x512	Color (24 bits/pixel)
Testing	Tree – 4.1.06	256x256	Color (24 bits/pixel)
Testing	Jelly beans – 4.1.08	256x256	Color (24 bits/pixel)
Testing	Female – 4.1.04	256x256	Color (24 bits/pixel)
Training	35010.jpg	481x321	Color (24 bits/pixel)
Training	95006.jpg	481x321	Color (24 bits/pixel)
Training	112082.jpg	481x321	Color (24 bits/pixel)
Training	124084.jpg	481x321	Color (24 bits/pixel)
Training	140055.jpg	481x321	Color (24 bits/pixel)
Training	156079.jpg	481x321	Color (24 bits/pixel)
Training	169012.jpg	481x321	Color (24 bits/pixel)
Training	189003.jpg	481x321	Color (24 bits/pixel)
Training	232038.jpg	481x321	Color (24 bits/pixel)
Training	317080.jpg	481x321	Color (24 bits/pixel)

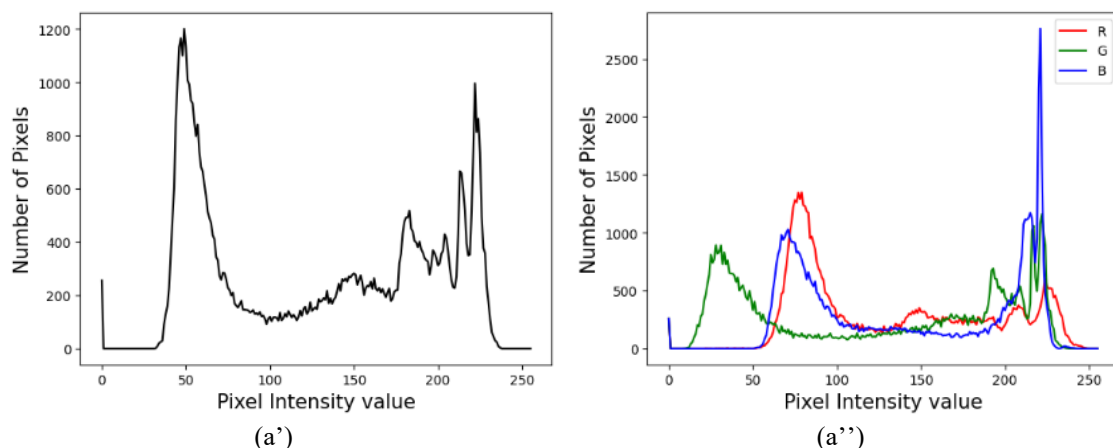


Figure 3. One of the benchmarks (RGB) test image data used to evaluate the method's performance came from the USC-SIPI image database. The images have their own RGB histogram (a'') and grayscale histogram (a') with (a) House – 4.1.05

¹ <https://www2.eecs.berkeley.edu/Research/Projects/CS/vision/bsds/>

² <https://sipi.usc.edu/database/>

2.2 Classical GWO vs IGWO

Mirjalili et al. (2014) [10] introduced the Grey Wolf Optimizer (GWO) as a metaheuristic algorithm inspired by the hunting habits and hierarchical social structure of grey wolves. These wolves typically form packs of 5-12 individuals, adhering to a strict social hierarchy composed of alpha (α), beta (β), delta (δ), and omega (ω) ranks [6]. In the mathematical formulation of GWO, the α , β , and δ wolves are designated as the first, second, and third-best solutions, respectively, guiding the optimization process. In contrast, the remaining ω wolves follow their lead [6]. The encirclement of prey is modeled by Equations 1, 2, and 3, where $\overrightarrow{X_{prey}}^{(t)}$ is the prey's position and $\overrightarrow{X_I}^{(t)}$ is the wolf's position. The control parameter linearly decreases from 2 to 0 (Equation 4), while \vec{r}_1 and \vec{r}_2 are random vectors in [0,1] [11]. All other wolves update their positions based on the superior knowledge of the α , β , and δ wolves (Equations 5 and 6). Vectors \vec{A}_i and \vec{C}_i manage the balance between exploration and exploitation: $|\vec{A}^{(t)}| < 1$ and/or $|\vec{C}^{(t)}| < 1$, signifies attacking the prey (exploitation), while $|\vec{A}^{(t)}| > 1$ and/or $|\vec{C}^{(t)}| > 1$ indicates exploration of new search areas to avoid local optima [6], [11]. This dynamic adjustment of a in each iteration effectively balances these two operators.

$$\overrightarrow{X_I}^{(t+1)} = \overrightarrow{X_{prey}}^{(t)} - \vec{A} \cdot \left| \vec{C} \cdot \overrightarrow{X_{prey}}^{(t)} - \overrightarrow{X_I}^{(t)} \right| \quad (1)$$

$$\vec{A} = 2\vec{a} \cdot \vec{r}_1 - \vec{a} \quad (2)$$

$$\vec{C} = 2 \cdot \vec{r}_2 \quad (3)$$

$$\vec{a} = 2 \left(1 - \frac{t}{T} \right) \quad (4)$$

The Inspired Grey Wolf Optimizer (IGWO) was proposed to address limitations of traditional GWO in real-world optimization [11], [12]. It incorporates individual and global best positions into its update process, addressing premature convergence or entrapment in local optima. This nonlinear adjustment strategy enhances the optimization process.

$$\overrightarrow{X_1}^{(t)} = \overrightarrow{X_{alpha}}^{(t)} - \vec{A}_1 \cdot \left| \vec{C}_1 \cdot \overrightarrow{X_{alpha}}^{(t)} - \overrightarrow{X_I}^{(t)} \right| \quad (5)$$

$$\overrightarrow{X_2}^{(t)} = \overrightarrow{X_{beta}}^{(t)} - \vec{A}_2 \cdot \left| \vec{C}_2 \cdot \overrightarrow{X_{beta}}^{(t)} - \overrightarrow{X_I}^{(t)} \right|$$

$$\overrightarrow{X_3}^{(t)} = \overrightarrow{X_{delta}}^{(t)} - \vec{A}_3 \cdot \left| \vec{C}_3 \cdot \overrightarrow{X_{delta}}^{(t)} - \overrightarrow{X_I}^{(t)} \right|$$

$$\overrightarrow{X_I}^{(t+1)} = \frac{\overrightarrow{X_1}^{(t)} + \overrightarrow{X_2}^{(t)} + \overrightarrow{X_3}^{(t)}}{3} \quad (6)$$

IGWO enhances GWO through two primary modifications. Firstly, it replaces the linear decay of parameter a with a logarithmic decay method, calculated by Equation 7. This non-linear adjustment aims to achieve a better balance between exploration and exploitation, facilitating convergence to the global optimum [12]. Secondly, IGWO modifies the equation for updwolf position vector. Unlike conventional GWO, which relies only on α , β , and δ wolves (Equations 5 and 6), IGWO incorporates each wolf's best individual position ($\overrightarrow{X_{pbest,I}}^{(t)}$) and the global best position ($\overrightarrow{X_{alpha}}^{(t)}$) as shown in Equation 8. This modification, inspired by PSO, enhances the algorithm's ability to avoid local optima. Coefficients c_1 and c_2 represent individual memory and population communication, respectively (both in [0,1]), with \vec{r}_3 and \vec{r}_4 as random vectors in [0,1]. Furthermore, similar to PSO, IGWO includes an inertia weight (ω), which linearly declines from an initial ($\omega_{initial}$) to a final (ω_{final}) value, as defined by Equation (9).

$$\vec{a}_t = \vec{a}_{initial} - (\vec{a}_{initial} - \vec{a}_{final}) \times \log\left(1 + (e - 1) \times \frac{t}{T_{max}}\right) \quad (7)$$

$$\vec{X}_I^{(t+1)} = \omega \cdot \left(\frac{X_1^{(t)} + X_2^{(t)} + X_3^{(t)}}{3}\right) + c_1 \cdot \vec{r}_3 \cdot (\vec{X}_{pbest,1}^{(t)} - \vec{X}_I^{(t)}) + c_2 \cdot \vec{r}_4 \cdot (\vec{X}_{alpha}^{(t)} - \vec{X}_I^{(t)}) \quad (8)$$

$$\omega_t = \left(\frac{T_{max} - t}{T_{max}}\right) \times (\omega_{initial} - \omega_{final}) + \omega_{final} \quad (9)$$

2.3 M. Masi Entropy for Multilevel Thresholding in Color Image Segmentation

M. Masi Entropy is an objective criterion used to determine the optimal thresholds in multilevel color image segmentation (ML-ISP). An RGB color image is defined as a 3D array of size $R \times K \times 3$, consisting of red (C_i^r), green (C_i^g), and blue (C_i^b) color channels. The purpose of multilevel thresholding is to find m optimal thresholds, namely $\{t_1, t_2, \dots, t_m\}$ that divide the image into $m + 1$ areas based on predefined criteria, such as M. Masi Entropy, Kapur Entropy, or the Otsu Method.

$F_{Masi}(t_1, t_2, \dots, t_m)$ measures segmentation quality by maximizing the variance within each image segment. The value of F_{Masi} is calculated by summing the M. Masi Entropy values (MME_j) from each divided segment according to Equation (10). Each MME_j is calculated using Equation (11), while the value φ_j is the pixel probability distribution in the j -th segment, which is calculated using Equation (12). The value $P_z^{(i)}$ in Equation (12) is the probability that the z -th gray level occurs at C_i^x and is calculated using Equation (13). The value of α in these equations is typically experimented on in the interval -1 to 3 with a step of 0.1 , and values of $\alpha < 1$ have shown steady and high quality. The best segmented image is the one that yields the highest F_{Masi} score among all possible threshold combinations.

$$F_{Masi}(t_1, t_2, \dots, t_m) = \sum_{j=0}^m MME_j = MME_0 + MME_1 + \dots + MME_m \quad (10)$$

$$MME_j = \frac{\log(1 - (1 - \alpha) \times j)}{(1 - \alpha)} \quad (11)$$

$$\varphi_m = \sum_{z=t_m}^{L-1} \frac{P_z^{(i)}}{w_m} \log\left(\frac{P_z^{(i)}}{w_m}\right), w_m = \sum_{z=t_m}^{L-1} P_z^{(i)} \quad (12)$$

$$P_j^{(i)} = \frac{n_j}{N_i}, (0 \leq P_j^{(i)} \leq 1) \wedge (\sum_{k=0}^{L-1} P_k^{(i)} = 1) \quad (13)$$

2.4 IGWO for Solving ML-ISP

Code 1 presents the pseudocode for implementing the IGWO to solve the ML-ISP. This study uses the IGWO method to determine optimal threshold values, represented by the wolf's vector position, at the m -th level for segmenting images into up to $m + 1$ distinct regions. The process takes the image's histogram as its input, and its output is the alpha wolf's position vector at the final iteration ($\vec{X}_{alpha}^{(T_{max})}$), corresponding to the derived optimal threshold values.

Code 1. IGWO with M. Masi Entropy to determine the m optimum thresholds

Input:

$N_{wolf} \leftarrow$ wolves population size
 $T_{max} \leftarrow$ maximum iteration
 $F_{func} \leftarrow$ M. Masi Entropy, Otsu Method, or Kapur Entropy

Output: Best individual solution at final iteration $\vec{X}_{alpha}^{(T_{max})}$ and best individual solution's fitness $Fit(\vec{X}_{alpha}^{(T_{max})})$

Initialization:

$GreyWolfs \leftarrow$ Initialize 2D matrix using Equation 14 of N_{wolf} grey wolf position.

F_{func} is used to calculate each individual fitness

Find $\vec{X}_{alpha}^{(0)}$, $\vec{X}_{beta}^{(0)}$, dan $\vec{X}_{delta}^{(0)}$

FOR t in range $(0, T_{max})$ **DO**

Use Equation 7. to update \vec{a}

```

FOR individual in GreyWolfs DO
    Use Equation 2 and 3 to update  $\vec{A}_x$  and  $\vec{C}_x$  respectively.
    Use Equation 5 to calculate  $\vec{X}_1^{(t)}, \vec{X}_2^{(t)}, \vec{X}_3^{(t)}$ 
    Use Equation 8 to update  $\vec{X}_I^{(t)}$ 
    Use Equation 15 to update  $\vec{X}_I^{(t)}$  boundaries solution space
ENDFOR
Update each individual fitness value using  $F_{func}$ 
Update  $\vec{X}_{alpha}^{(t)}, \vec{X}_{beta}^{(t)},$  dan  $\vec{X}_{delta}^{(t)}$ 
ENDFOR
Return  $\vec{X}_{alpha}^{(T_{max})}, Fit(\vec{X}_{alpha}^{(T_{max})})$ 
    
```

Equation 14 is used to initialize the positional vector representation of each i -th wolf, which is expressed as \vec{X}_I . N_{wolf} represents the total number of wolves that were initiated. The gray level of an image represents the threshold value, which is $x_{(I,k)} \in \vec{X}_I^{(t)}$. All wolves' fitness is determined at the start of the iteration ($t = 0$) using a preset objective function, specifically the Otsu method, Kapur Entropy, or M. Masi Entropy [9]. Next, we define three wolves with optimal fitness values at initial as follows: $\vec{X}_{alpha}^{(0)}, \vec{X}_{beta}^{(0)},$ dan $\vec{X}_{delta}^{(0)}$. Each wolf uses Equation 8 to update its position based on IGWO's new formulation for each iteration during a predefined maximum iteration T_{max} . Vector \vec{A} , vector \vec{C} , and vector \vec{a} are determined using Equations 2, 3, and 7, respectively, prior to the positions being updated.

$$\vec{X}_I^{(0)} = [x_{(I,1)}, x_{(I,2)}, \dots, x_{(I,m)}], (I = 1, 2, \dots, N) \wedge (0 < x_{(I,1)} \dots < x_{(I,m)} < L) \quad (14)$$

$$x_{(I,k)} = randInt(0, (L - 1)) \quad (15)$$

$$\vec{X}_I^{(t+1)} = \begin{cases} L - round(random(0,1) * randomInteger(0, L)), & (x_{(I,k)}) > L \\ 0, & (x_{(I,k)}) < 0 \\ x_{(I,k)}, & otherwise \end{cases}, \forall x_{(I,k)} \in \vec{X}_I^{(t+1)}$$

When the value $x_{(J,k)}$ is outside the range of gray level G , the updated vector $\vec{X}_I^{(t+1)}$ may not be inside the bounds of ML-ISP. Consequently, $\vec{X}_I^{(t+1)}$ is adjusted to be in the problem solution space in this study using Equation 15. Then, using the same formula as when $t = 0$, the fitness value of each j -th agent is expressed as $Fit(\vec{X}_I)$.

2.5 Segmenting Images with the Best Threshold

Each channel in the test image is then segmented using the optimal threshold determined by the IGWO-based optimization procedure. Using the pseudocode shown in Algorithm 3 from prior research [9], the C_i^x image is partitioned into $m + 1$ regions using an optimal $\{t_1, t_2, \dots, t_m\}$. S_i^{RGB} for RGB color images, and S_i^{gray} for grayscale images are the representations of the C_i^x image segmented with the ideal m threshold.

S_i^{RGB} is obtained by merging the segmentation results from $C_i^r, C_i^g,$ and C_i^b . Assume $m_r, m_g,$ and m_b as the thresholding levels for each of the RGB image's $r, g,$ and b channels. The optimal threshold for each channel is determined using the SI method. Using the pseudocode shown in Algorithm 3 from prior research [9], each channel is segmented using the optimal threshold. Each channel's segmented picture is represented by $S_i^r, S_i^g,$ and S_i^b , such that $S_i^{RGB} = [S_i^r, S_i^g, S_i^b]$. Thus, S_i^{RGB} has less color levels than C_i^{RGB} and has the most $m_r \times m_g \times m_b$ [13].

2.6 Environmental and Experiment Setup

The performance stability of the suggested IGWO for ML-ISP was assessed through experiments using three objective functions: M. Masi Entropy, the Otsu method, and Kapur Entropy. To ensure a fair comparison, all methods used consistent stopping criteria, including a maximum of 100 iterations, a population size of 25 solutions, and 30 trials per method [5]. Consistent with prior research [1], [2], test images were evaluated for 2, 3, 4, and 5 thresholds. All algorithms were implemented and executed using Python v3.8.5 on a Windows 10 (64-bit) environment, powered by an AMD Ryzen AI HX 370 w/ Radeon 890M @2000 Mhz and 32GB of RAM.

To determine the optimal hyperparameter combination for each method, a *GridSearch* technique was employed. This systematic approach explores all possible hyperparameter value combinations within a defined search space (Table 2) to identify the configuration that yields the best results. The optimization metric used for hyperparameter tuning was the average fitness value across all training data, specifically for five thresholds using the M. Masi Entropy as the fitness function. For IGWO, tuned parameters included the population communication coefficient (c_1), individual memory coefficient (c_2), initial inertia weight ($\omega_{initial}$), and final inertia weight (ω_{final}).

Table 2. List of hyperparameters along with the solution space for IGWO method

No	Parameter	Search space
1	Population communication coefficient (c_1)	[0.1, 0.3, 0.5, 0.7, 0.9]
2	Individual memory coefficient (c_2)	[0.2, 0.4, 0.6, 0.8, 1]
3	Initial value of vector \vec{a}	[1,2]
4	Initial value of inertia weight ($\omega_{initial}$)	[0.5, 0.7, 0.9]
5	Final value of inertia weight (ω_{final})	[0.1]

2.7 Evaluation Metrics

Both qualitative and quantitative methods were utilized to evaluate the segmented images. Qualitative assessment involved visual comparison between the original and segmented images at each threshold level. The quantitative evaluation was conducted using six primary metrics: Peak Signal-to-Noise Ratio (PSNR), Universal Quality Index (UQI), and Structural Similarity Index Metric (SSIM). In essence, PSNR uses an image's pixel intensity value to determine the difference between S_i and C_i . Equation 16 is used to determine the PSNR, while Equation 17 is used to determine the MSE value. $S_{(x,y)}$ represents the gray level pixels at the coordinates (x, y) of the segmented image, whereas $C_{(x,y)}$ represents the original image's gray level pixels.

SSIM (Equation 18) and UQI (Equation 19) assess structural similarities, brightness, and distortion, providing a more comprehensive quality measure than PSNR alone [7]. The average intensity values of C_i and S_i are represented by the μ_C and μ_S values, respectively. The standard deviations of C_i and S_i are represented by the values of σ_C and σ_S , respectively. The covariance between C_i and S_i is defined by the value of $cov_{(C,S)}$. The values of a and b are constant at 6.5025 and 58.52252, respectively.

$$PSNR_{(C,S)} = 10 \log_{10} \left(\frac{255 \times 255}{MSE_{(C,S)}} \right) \quad (16)$$

$$MSE_{(C,S)} = \frac{\sum_{x=1}^R \sum_{y=1}^K |S_{(x,y)} - C_{(x,y)}|}{R \times K} \quad (17)$$

$$SSIM_{(C,S)} = \frac{(2\mu_S\mu_C + a)(2cov_{(C,S)} + b)}{(\mu_C^2 + \mu_S^2 + a)(\sigma_C^2 + \sigma_S^2 + b)} \quad (18)$$

$$UQI_{(C,S)} = \frac{4cov_{(C,S)}\mu_C\mu_S}{(\mu_C^2 + \mu_S^2)(\sigma_C^2 + \sigma_S^2)} \quad (19)$$

3. Results and Discussion

Using *GridSearch* to select the best hyperparameter combinations in IGWO, $c_1 = 0.9$, $c_2 = 1$, $\omega_{initial} = 0.7$, $\omega_{final} = 0.1$, dan $\vec{a}_{initial} = 1$ were found to have an average fitness value of 2870.383, an average PSNR of 19.244, an average SSIM of 0.8145, and an average UQI of 0.888. An IGWO model with three objective functions—the M. Masi Entropy, Kapur Entropy, and Otsu Method—is then created using the optimal hyperparameter combination.

This section thoroughly evaluates the IGWO for multilevel color image segmentation (ML-ISP), using both quantitative and qualitative assessments. The performance, measured by PSNR, SSIM, and UQI metrics, along with visual inspection, consistently shows that the IGWO framework, combined with the M. Masi Entropy objective function, provides superior segmentation results across most test images and threshold levels. A detailed analysis of the quantitative metrics in Table 3 reveals distinct trends. For instance, the IGWO-M. Masi Entropy configuration frequently achieves the highest PSNR values, especially as the number of thresholds increases, as seen in "*Female – 4.1.04*" and "*Mandrill (a.k.a. Baboon) – 4.2.03*". IGWO-M. Masi Entropy consistently outperforms in all m configurations, yielding PSNRs of 10.303, 10.380, 10.510, and 10.579, respectively. While IGWO-Otsu shows competitive performance at lower thresholds for some images, IGWO-Kapur Entropy generally exhibits lower PSNR values, except for "*Splash – 4.2.01*" at $m = 2$.

Further analysis of the SSIM and UQI metrics in Table 3 largely confirms the superiority of IGWO with M. Masi Entropy. For images like "*Jelly beans – 4.1.08*" and "*Mandrill (a.k.a. Baboon) – 4.2.03*," M. Masi Entropy consistently yields the highest values across all threshold levels, indicating better preservation of structural information and overall image quality. For example, "*Jelly beans – 4.1.08*" achieves an SSIM of 0.762 and UQI of 0.861 with IGWO-M. Masi Entropy at $m = 5$. Conversely, while generally underperforming, IGWO-Kapur Entropy demonstrates exceptional results for "*Splash – 4.2.01*," leading across all SSIM and UQI values, which suggests its specific suitability for certain image characteristics. These comprehensive quantitative findings highlight the robust and adaptable performance of IGWO when optimized with the appropriate objective functions for challenging ML-ISP tasks.

Table 3. Mean PSNR, SSIM, and UQI values for all test images

Test Images	m	IGWO Otsu Method			IGWO Kapur Entropy			IGWO M. Masi Entropy		
		PSNR	SSIM	UQI	PSNR	SSIM	UQI	PSNR	SSIM	UQI
Female – 4.1.04	2	9.998	0.506	0.785	9.379	0.484	0.773	9.706	0.495	0.776
	3	10.506	0.531	0.821	9.774	0.513	0.801	10.898	0.550	0.831
	4	11.303	0.569	0.850	10.315	0.542	0.825	11.056	0.559	0.844
	5	11.070	0.568	0.850	10.809	0.572	0.844	11.229	0.568	0.853
House – 4.1.05	2	8.428	0.506	0.767	7.972	0.483	0.745	8.575	0.508	0.771
	3	10.199	0.568	0.830	8.476	0.504	0.772	9.608	0.546	0.811
	4	9.831	0.554	0.821	9.313	0.533	0.803	9.975	0.554	0.824
	5	10.380	0.573	0.840	9.368	0.539	0.810	10.677	0.586	0.850
Tree – 4.1.06	2	12.262	0.642	0.852	11.702	0.607	0.847	11.843	0.617	0.839
	3	12.639	0.665	0.872	12.475	0.658	0.876	12.619	0.666	0.874
	4	12.906	0.681	0.882	12.402	0.660	0.880	13.286	0.704	0.893
	5	13.456	0.716	0.900	12.638	0.677	0.888	13.344	0.706	0.896
Jelly beans – 4.1.08	2	10.261	0.737	0.844	9.471	0.691	0.818	10.303	0.742	0.845
	3	10.360	0.745	0.851	9.946	0.713	0.838	10.380	0.748	0.851
	4	10.504	0.755	0.859	10.056	0.721	0.843	10.510	0.759	0.858
	5	10.524	0.759	0.861	10.141	0.728	0.847	10.579	0.762	0.861
Splash – 4.2.01	2	12.878	0.587	0.796	13.033	0.605	0.828	13.017	0.592	0.796
	3	14.159	0.630	0.828	14.054	0.641	0.866	14.199	0.626	0.836
	4	14.785	0.644	0.864	14.717	0.681	0.887	14.552	0.642	0.851
	5	15.231	0.674	0.882	14.624	0.690	0.889	15.083	0.662	0.875
Mandrill (a.k.a. Baboon) – 4.2.03	2	9.860	0.490	0.791	9.178	0.454	0.767	9.816	0.489	0.790
	3	10.539	0.533	0.820	9.746	0.493	0.796	10.539	0.535	0.823
	4	10.849	0.550	0.834	10.046	0.509	0.808	10.883	0.554	0.836
	5	11.224	0.572	0.848	10.211	0.520	0.818	11.426	0.580	0.853

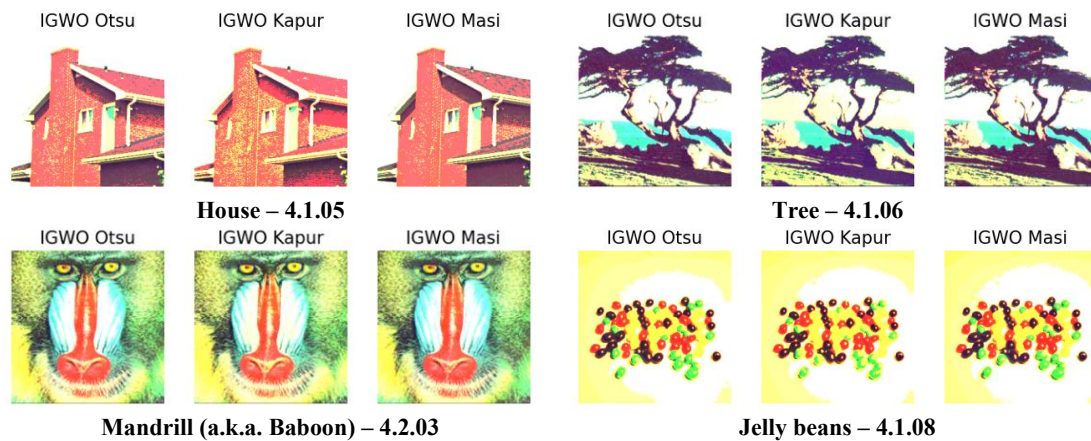


Figure 4. Results of 3-level segmented RGB test images from IGWO using Kapur Entropy, Otsu Method, and M. Masi Entropy

The quantitative findings, supported by higher PSNR, SSIM, and UQI values, were visually confirmed by qualitative results presented in segmented images (Figure 4). Visual inspection of the 3-level segmented RGB test images revealed that segmentations generated with the M.Masi Entropy objective function consistently produced more precise boundaries, more distinct regions, and a better overall representation of the original image's semantic content than those generated with the Otsu method or Kapur Entropy. For example, images like "*Mandrill (a.k.a. Baboon) – 4.2.03*" and "*Jelly beans – 4.1.08*," which had higher quantitative metrics with M. Masi Entropy, also appeared more visually coherent and had less over-segmentation. This strong correlation between quantitative metrics and visual outputs affirms that the Inspired Grey Wolf Optimizer (IGWO), especially with M. Masi Entropy, effectively captures essential image features. The experimental results demonstrate that the M. Masi Entropy objective function provides superior, stable performance across diverse benchmark images and varying threshold levels, establishing the IGWO and M. Masi Entropy combination as a robust solution for challenging multilevel color image segmentation tasks.

Table 4. Additional test data for benchmarking our proposed IGWO and M. Masi Entropy

Type	Filename	Dimension (pixels)	Colospace
Testing	Sailboat on lake – 4.2.06	512x512	Color (24 bits/pixel)
Testing	Peppers – 4.2.07	512x512	Color (24 bits/pixel)
Testing	House	512x512	Color (24 bits/pixel)
Testing	249061.jpg	481x321	Color (24 bits/pixel)
Testing	247085.jpg	481x321	Color (24 bits/pixel)
Testing	173036.jpg	481x321	Color (24 bits/pixel)
Testing	76002.jpg	481x321	Color (24 bits/pixel)
Testing	68077.jpg	481x321	Color (24 bits/pixel)

To evaluate the effectiveness of the IGWO and M. Masi Entropy combination for ML-ISP, eight additional test datasets from BSDS300 and USC-SIPI were used, as shown in Table 4. The image data were selected based on their diverse, multimodal pixel intensity distributions across the R, G, and B channels, which are similar to the histogram distributions of the benchmark images shown in Figure 3. As summarized in Table 5, the IGWO model, when integrated with the M. Masi Entropy objective function, consistently achieved higher average PSNR and UQI scores than the Kapur Entropy of Entropy function and the Otsu Method. This reinforces the model's resilience, as demonstrated by earlier findings. Additionally, qualitative inspection of 2-level segmented RGB images from the supplementary test set (Figure 5) showed that M. Masi Entropy on IGWO provides a better overall representation of the original image's semantic

content, with more distinct regions and more precise edges than images generated by the Otsu method or Kapur Entropy.

Table 5. Mean PSNR and UQI values for all test images

Test Images	m	IGWO Otsu Method		IGWO Kapur Entropy		IGWO M. Masi Entropy	
		PSNR	UQI	PSNR	UQI	PSNR	UQI
173036.jpg	2	7.621	0.619	7.540	0.615	12.037	0.751
	3	8.850	0.695	8.428	0.678	12.165	0.793
	4	10.664	0.770	9.851	0.748	14.416	0.853
	5	12.166	0.825	11.579	0.809	14.294	0.872
247085.jpg	2	7.877	0.685	7.695	0.677	9.217	0.756
	3	9.097	0.756	9.071	0.756	9.697	0.789
	4	9.488	0.782	9.338	0.777	10.052	0.809
	5	9.712	0.798	9.790	0.800	10.245	0.820
249061.jpg	2	8.981	0.797	8.907	0.793	9.291	0.809
	3	9.593	0.819	9.317	0.810	9.757	0.826
	4	10.019	0.836	10.131	0.839	10.179	0.843
	5	10.185	0.842	10.410	0.849	10.664	0.858
Sailboat on lake – 4.2.06	2	11.287	0.804	10.804	0.791	10.134	0.782
	3	11.414	0.828	11.913	0.841	10.991	0.822
	4	12.432	0.863	12.189	0.856	11.485	0.843
	5	12.284	0.866	12.613	0.875	11.563	0.854
Peppers – 4.2.07	2	9.554	0.708	9.748	0.714	10.353	0.746
	3	10.091	0.745	9.917	0.739	10.642	0.772
	4	10.875	0.787	11.094	0.794	10.928	0.795
	5	11.477	0.810	11.171	0.805	11.368	0.815
68077.jpg	2	9.455	0.768	9.212	0.758	8.591	0.740
	3	10.141	0.798	10.515	0.809	11.048	0.833
	4	11.079	0.831	10.777	0.823	10.930	0.834
	5	11.810	0.852	11.853	0.858	11.604	0.854
76002.jpg	2	10.524	0.693	10.508	0.696	10.674	0.699
	3	11.141	0.753	11.250	0.757	11.580	0.765
	4	11.508	0.787	11.771	0.795	12.280	0.801
	5	11.809	0.812	11.905	0.813	12.317	0.822
House	2	10.256	0.835	10.329	0.836	9.962	0.828
	3	10.755	0.855	10.918	0.860	10.287	0.842
	4	10.792	0.860	11.164	0.870	10.411	0.850
	5	11.270	0.874	11.182	0.872	10.526	0.855

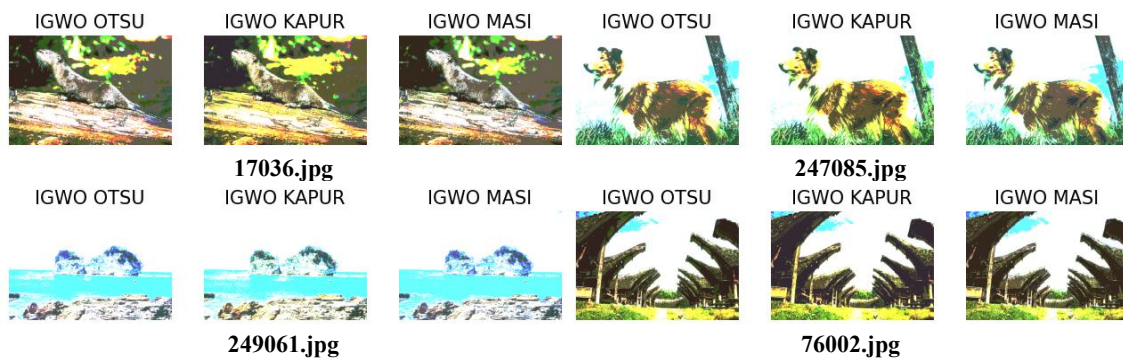


Figure 5. Results of 2-level segmented RGB additional test images from IGWO using Kapur Entropy, Otsu Method, and M. Masi Entropy

4. Conclusion and Future Works

This research introduces and evaluates an Inspired Grey Wolf Optimizer (IGWO) for multilevel image segmentation (ML-ISP) specifically for RGB color images. The study addresses the limitations of prior work by assessing IGWO's performance alongside M. Masi Entropy and

other baseline methods, such as Kapur Entropy and the Otsu Method. Experimental results from rigorous quantitative (PSNR, SSIM, UQI) and qualitative analyses consistently show that the M. Masi Entropy objective function, when integrated with IGWO, delivers superior segmentation performance across most benchmark images and various threshold levels. This enhanced performance, attributed to IGWO's improved exploration-exploitation balance, confirms its robustness for challenging ML-ISP on color images.

Future work could explore the application of IGWO with other advanced objective functions or investigate its integration with deep learning frameworks to further enhance segmentation capabilities and computational efficiency.

References

- [1] B. S. Khehra, A. Singh, and L. Kaur, "M. Masi Entropy- and Grey Wolf Optimizer-Based Multilevel Thresholding Approach for Image Segmentation," *Journal of The Institution of Engineers (India): Series B*, vol. 103, no. 5, pp. 1619–1642, Oct. 2022, doi: 10.1007/s40031-022-00740-8.
- [2] G. Ma and X. Yue, "An improved whale optimization algorithm based on multilevel threshold image segmentation using the Otsu method," *Engineering Applications Artificial Intelligence*, vol. 113, Aug. 2022, doi: 10.1016/j.engappai.2022.104960.
- [3] P. Upadhyay and J. K. Chhabra, "Multilevel thresholding based image segmentation using new multistage hybrid optimization algorithm," *Journal of Ambient Intelligence Humanized Computing*, vol. 12, no. 1, pp. 1081–1098, Jan. 2021, doi: 10.1007/s12652-020-02143-3.
- [4] K. P. Baby Resma and M. S. Nair, "Multilevel thresholding for image segmentation using Krill Herd Optimization algorithm," *Journal of King Saud University - Computer and Information Sciences*, vol. 33, no. 5, pp. 528–541, Jun. 2021, doi: 10.1016/j.jksuci.2018.04.007.
- [5] M. A. El Aziz, A. A. Ewees, and A. E. Hassanien, "Whale Optimization Algorithm and Moth-Flame Optimization for multilevel thresholding image segmentation," *Expert Systems with Applications*, vol. 83, pp. 242–256, Oct. 2017, doi: 10.1016/j.eswa.2017.04.023.
- [6] A. K. M. Khairuzzaman and S. Chaudhury, "Multilevel thresholding using grey wolf optimizer for image segmentation," *Expert Systems with Applications*, vol. 86, pp. 64–76, Nov. 2017, doi: 10.1016/j.eswa.2017.04.029.
- [7] M. Abdel-Basset, V. Chang, and R. Mohamed, "HSMA_WOA: A hybrid novel Slime mould algorithm with whale optimization algorithm for tackling the image segmentation problem of chest X-ray images," *Applied Soft Computing Journal*, vol. 95, Oct. 2020, doi: 10.1016/j.asoc.2020.106642.
- [8] A. K. M. Khairuzzaman and S. Chaudhury, "Masi entropy based multilevel thresholding for image segmentation," *Multimedia Tools and Applications*, vol. 78, no. 23, pp. 33573–33591, Dec. 2019, doi: 10.1007/s11042-019-08117-8.
- [9] I. M. S. Bimantara and A. Yuniarti, "Multilevel Thresholding of Color Image Segmentation Using Memory-based Grey Wolf Optimizer With Otsu Method, Kapur, and M.Masi Entropy," *Jurnal Nasional Pendidikan Teknik Informatika (JANAPATI)*, vol. 12, no. 2, pp. 304–337, Aug. 2023, doi: 10.23887/janapati.v12i2.62874.
- [10] S. Mirjalili, S. M. Mirjalili, and A. Lewis, "Grey Wolf Optimizer," *Advances in Engineering Software*, vol. 69, pp. 46–61, 2014, doi: 10.1016/j.advengsoft.2013.12.007.
- [11] S. Gupta and K. Deep, "A memory-based Grey Wolf Optimizer for global optimization tasks," *Applied Soft Computing Journal*, vol. 93, Aug. 2020, doi: 10.1016/j.asoc.2020.106367.
- [12] W. Long, J. Jiao, X. Liang, and M. Tang, "Inspired grey wolf optimizer for solving large-scale function optimization problems," *Applied Mathematical Modelling*, vol. 60, pp. 112–126, Aug. 2018, doi: 10.1016/j.apm.2018.03.005.
- [13] S. Borjigin and P. K. Sahoo, "Color image segmentation based on multi-level Tsallis-Havrda-Charvát entropy and 2D histogram using PSO algorithms," *Pattern Recognition*, vol. 92, pp. 107–118, Aug. 2019, doi: 10.1016/j.patcog.2019.03.011.